

STRUCTURE-PHOTOCATALYTIC ACTIVITY RELATIONSHIP OF CARBON  
DOPED TITANIUM DIOXIDE ANALYZED BY DENSITY FUNCTIONAL  
THEORY AND FUZZY LOGIC GRAPH

SITI HAJAR BINTI ALIAS

UNIVERSITI TEKNOLOGI MALAYSIA

STRUCTURE-PHOTOCATALYTIC ACTIVITY RELATIONSHIP OF CARBON  
DOPED TITANIUM DIOXIDE ANALYZED BY DENSITY FUNCTIONAL  
THEORY AND FUZZY LOGIC GRAPH

SITI HAJAR BINTI ALIAS

A thesis submitted in fulfilment of the  
requirements for the award of the degree of  
Doctor of Philosophy

Faculty of Science  
Universiti Teknologi Malaysia

JULY 2020

## DEDICATION

To my beloved husband, Mohammad Lutfi bin Mohd Afandi,  
late father, Hj Alias bin Hj Sulaiman, mother, Hjh Normah binti Hj Ab Karim,  
mother-in-law, Junaidah Deraman, son, Muhammad Iskandar Zulkarnain bin  
Mohammad Lutfi and all family members for their du'a, love, support,  
encouragements and advices.

*Al-fatihah to my late father, Hj Alias bin Hj Sulaiman, and my late father-in-law,  
Mohd Afandi bin Mohd Noor*

## ACKNOWLEDGEMENT

My utmost gratitude belongs to Allah S.W.T for giving me the strength and wisdom to complete this research.

In preparing this thesis, I was in contact with many people, researchers, and academicians, who contributed to my understanding and thoughts. In particular, I wish to express my sincere appreciation to my main supervisor, Professor Dr. Hadi Nur, for encouragement, guidance, critics, motivation and friendship. I am also very thankful to my co-supervisor Dr. Sheela Chandren for her guidance, advice and motivation. This thesis would not have been the same as presented here without their continued support and involvement. My sincere gratitude also goes to Dr. Riadh Sahnoun, Dr. Fazira Illyana Mohd Razak and Prof. Dr. Daud Mohamad for the assistance and valuable academic insight.

I am also indebted to Universiti Teknologi MARA (UiTM) and Ministry of Higher Education Malaysia for funding my Ph.D study under SLAB/SLAI programme. All laboratory officers and research officers from Ibnu Sina Institute for Fundamental Science Studies and UPMU, UTM also deserve special thanks for their assistance.

I do extend my sincere appreciation to all my colleagues and others who have supported on various occasions. Indeed, their views and tips are beneficial. Last but not least, I am grateful to all my family member for their continuous support, prayer, understanding, love, advices and encouragement for me to complete my research.

## ABSTRACT

Carbon doping is a promising way to modify the properties of TiO<sub>2</sub> for enhancing its photocatalytic performance. Although there are many publications about the enhancement of photocatalytic activity of TiO<sub>2</sub>, the relationship between the structural and physical properties with the photocatalytic activity of TiO<sub>2</sub> is still not clearly understood. A new approach has been proposed to evaluate the structure-photocatalytic activity relationship with the aim to better understand the dominant properties that determine the photocatalytic activities of C-doped TiO<sub>2</sub>. Fuzzy logic graph has been used as a new approach in determining the dominant factor for the structure-photocatalytic activity relationship of C-doped TiO<sub>2</sub>. Characterization results from experimental study were used in the fuzzy logic graph. For the experimental study, two types of C-doped TiO<sub>2</sub> were successfully synthesized by the sol-gel method with addition of cetyltrimethylammonium bromide (CTAB) surfactant and without the addition of CTAB, at different calcination temperatures, to compare with commercial TiO<sub>2</sub>. The synthesized photocatalysts were characterized using several characterization techniques. Photooxidation of styrene with aqueous hydrogen peroxide has been used as the model reaction for organic pollutants to study the structure-photocatalytic activity relationship under UV and visible light irradiation. X-ray photoelectron spectroscopy (XPS) spectra show that C was doped into TiO<sub>2</sub>'s lattice with the amount of C of about 2.5 at% for CTAB-C/TiO<sub>2</sub>-500 samples and about 10.5 at% for C/TiO<sub>2</sub>-500 samples at interstitial and substitutional positions of anatase TiO<sub>2</sub>. Energy dispersive X-ray spectroscopy (EDX) and XPS results for CTAB-C/TiO<sub>2</sub> samples show a lower amount of C incorporated into TiO<sub>2</sub> as compared to C/TiO<sub>2</sub> without the addition of CTAB, which may be caused by the removal of C impurity by the CTAB surfactant. Furthermore, the effects of calcination temperature from 300 to 700°C on the physicochemical properties of the C-doped TiO<sub>2</sub> were also studied. Calcination temperature affected the phase, morphology, surface area, porosity, crystallite size and amount of C. The surface area of CTAB-C/TiO<sub>2</sub> and C/TiO<sub>2</sub> samples is shown to decrease as the calcination temperature increased. Additionally, the confirmation on the effect of C on the band gap energy of the anatase TiO<sub>2</sub> was investigated using density functional theory (DFT). Total density of states (TDOS) shows that the C affects the band gap energy of TiO<sub>2</sub> by introducing the mid gap states between the band gap. Based on DFT analysis and photocatalytic experiment, six physical properties have been chosen to be used for fuzzy logic graph, i.e. surface area, phase, amount of electron-hole recombine, band gap energy, existence of sub-band gap and amount of C. Fuzzy logic graph analysis shows that surface area is a dominant factor for the photooxidation of styrene under UV and visible light irradiations, followed by phase, amount of C and amount of electron-hole recombine. This study demonstrated that the combination of photocatalytic experiment, DFT and fuzzy logic graph analysis can be used to clarify the structure-photocatalytic activity relationship in TiO<sub>2</sub> photocatalytic systems.

## ABSTRAK

Pendopan karbon adalah cara yang menjanjikan dalam pengubahsuaian sifat  $\text{TiO}_2$  bagi meningkatkan prestasi fotopemangkinannya. Walaupun terdapat banyak penerbitan tentang peningkatan aktiviti fotopemangkinan  $\text{TiO}_2$ , hubungan antara sifat-sifat struktur dan fizik dengan aktiviti fotopemangkinan  $\text{TiO}_2$  masih belum difahami dengan jelas. Satu pendekatan baharu telah dicadangkan untuk menilai hubungan struktur-aktiviti fotopemangkinan dengan matlamat untuk memahami dengan lebih baik sifat-sifat dominan yang menentukan aktiviti fotopemangkinan  $\text{TiO}_2$  didopkan-C. Graf logik kabur telah digunakan sebagai pendekatan baharu dalam menentukan faktor dominan bagi hubungan struktur-aktiviti fotopemangkinan  $\text{TiO}_2$  didopkan-C. Keputusan pencirian daripada kajian eksperimen telah digunakan dalam graf logik kabur. Bagi kajian eksperimen, dua jenis  $\text{TiO}_2$  didopkan-C telah berjaya disintesis dengan menggunakan kaedah sol-gel dengan penambahan surfaktan setiltrimetilammonium bromida (CTAB) dan tanpa penambahan CTAB, pada suhu pengkalsinan yang berbeza untuk dibandingkan dengan  $\text{TiO}_2$  komersial. Fotomangkin yang disintesis telah dicirikan menggunakan beberapa teknik pencirian. Pengoksidaan stirena dengan hidrogen peroksida telah digunakan sebagai model tindak balas bagi bahan pencemar organik untuk mengkaji hubungan struktur-aktiviti fotopemangkinan di bawah sinaran UV dan cahaya nampak. Spektrum spektroskopi fotoelektron sinar-X (XPS) menunjukkan bahawa C telah terdopkan ke dalam kekisi  $\text{TiO}_2$  dengan jumlah C kira-kira 2.5 at% bagi sampel CTAB-C/ $\text{TiO}_2$ -500 dan kira 10.5 at% bagi sampel C/ $\text{TiO}_2$ -500 pada posisi di antara ruang dan posisi penggantian  $\text{TiO}_2$  anatas. Hasil spektroskopi serakan tenaga sinar-X (EDX) dan XPS bagi sampel CTAB-C/ $\text{TiO}_2$  menunjukkan jumlah C yang lebih rendah telah digabungkan ke dalam  $\text{TiO}_2$  berbanding C/ $\text{TiO}_2$  tanpa penambahan CTAB, yang mungkin disebabkan oleh penyingkiran bendasing C oleh surfaktan CTAB. Tambahan pula, kesan suhu pengkalsinan dari 300 hingga 700°C terhadap sifat fizikokimia  $\text{TiO}_2$  didopkan-C telah juga dikaji. Suhu pengkalsinan telah memberi kesan kepada fasa, morfologi, luas permukaan, keliangan, saiz hablur dan jumlah C. Luas permukaan sampel CTAB-C/ $\text{TiO}_2$  dan C/ $\text{TiO}_2$  menunjukkan ia telah berkurang apabila suhu pengkalsinan meningkat. Tambahan lagi, pengesahan kesan C terhadap tenaga luang jalur  $\text{TiO}_2$  anatas telah disiasat menggunakan teori ketumpatan berfungsi (DFT). Ketumpatan keadaan keseluruhan (TDOS) menunjukkan bahawa C mempengaruhi tenaga luang jalur  $\text{TiO}_2$  dengan memperkenalkan keadaan luang pertengahan di antara luang jalur. Berdasarkan analisis DFT dan eksperimen fotopemangkinan, enam sifat fizik telah dipilih untuk digunakan bagi graf logik kabur, iaitu luas permukaan, fasa, jumlah gabungan semula elektron-lubang, tenaga luang jalur, kewujudan luang sub-jalur dan jumlah C. Analisis graf logik kabur menunjukkan bahawa luas permukaan adalah faktor dominan bagi fotopengoksidaan stirena di bawah sinaran UV dan cahaya nampak, diikuti dengan fasa, jumlah C dan jumlah gabungan semula elektron-lubang. Kajian ini membuktikan bahawa gabungan eksperimen fotopemangkinan, DFT dan analisis graf logik kabur boleh digunakan untuk menjelaskan hubungan struktur-aktiviti fotopemangkinan dalam sistem fotopemangkinan  $\text{TiO}_2$ .

## TABLE OF CONTENTS

	TITLE	PAGE
	<b>DECLARATION</b>	<b>ii</b>
	<b>DEDICATION</b>	<b>iii</b>
	<b>ACKNOWLEDGEMENT</b>	<b>iv</b>
	<b>ABSTRACT</b>	<b>v</b>
	<b>ABSTRAK</b>	<b>vi</b>
	<b>TABLE OF CONTENTS</b>	<b>vii</b>
	<b>LIST OF TABLES</b>	<b>xi</b>
	<b>LIST OF FIGURES</b>	<b>xiii</b>
	<b>LIST OF ABBREVIATIONS</b>	<b>xvii</b>
	<b>LIST OF APPENDICES</b>	<b>xix</b>
<b>CHAPTER 1</b>	<b>INTRODUCTION</b>	<b>1</b>
1.1	Background of Study	1
1.2	Problem Statement	4
1.3	Objectives of Study	5
1.4	Scope of Study	6
1.5	Significance of Study	7
1.6	Research Outline	7
<b>CHAPTER 2</b>	<b>PHYSICOCHEMICAL AND ELECTRONIC PROPERTIES OF C-DOPED TiO<sub>2</sub> AND ITS PHOTOCATALYTIC ACTIVITY IN STYRENE OXIDATION UNDER UV AND VISIBLE LIGHT IRRADIATIONS</b>	<b>9</b>
2.1	Introduction	9
2.2	Photocatalysis	9
2.3	TiO <sub>2</sub> as Semiconductor Photocatalyst	11
2.3.1	Properties of TiO <sub>2</sub>	12
2.4	C-doped TiO <sub>2</sub> as Visible Light Photocatalyst	14
2.5	Synthesis of C-doped TiO <sub>2</sub>	16

2.6	Mechanism of Photocatalytic Reaction of TiO <sub>2</sub>	17
2.7	Structure-Photocatalytic Activity Relationship of TiO <sub>2</sub>	20
2.8	Experimental	25
2.8.1	Chemicals	25
2.8.2	Synthesis of C-doped TiO <sub>2</sub>	25
2.8.3	Characterization of Prepared Photocatalyst	26
2.8.3.1	X-ray Diffraction (XRD)	26
2.8.3.2	Field-Emission Scanning Electron Microscopy (FESEM) and Energy Dispersive X-Ray (EDX) Spectroscopy	27
2.8.3.3	Fourier Transform Infrared (FTIR) Spectroscopy	28
2.8.3.4	UV-Visible Diffuse Reflectance (UV-Vis DR) Spectrophotometer	28
2.8.3.5	Photoluminescence (PL) Spectroscopy	29
2.8.3.6	Total Specific Surface Area (BET) and Pore Volume Analysis	29
2.8.3.7	X-Ray Photoelectron Spectroscopy (XPS)	30
2.8.4	Photocatalytic Activity of Styrene with Aqueous Hydrogen Peroxide	30
2.9	Results and Discussion	32
2.9.1	Physicochemical Properties of C-doped TiO <sub>2</sub>	32
2.9.1.1	Chemical Composition	32
2.9.1.2	Crystal Phase and Crystallinity	33
2.9.1.3	Functional Groups	37
2.9.1.4	Morphology	41
2.9.1.5	Surface Area and Porosity Analysis	43
2.9.2	Optical Properties and Electronic Structure of C-doped TiO <sub>2</sub>	48
2.9.2.1	UV-Vis DR Spectroscopy	48
2.9.2.2	Photoluminescence	51
2.9.2.3	XPS	53



2.9.3	Photooxidation of Styrene	59
2.10	Summary	62
<b>CHAPTER 3 ELECTRONIC STRUCTURE OF ANATASE AND C-DOPED ANATASE TiO<sub>2</sub> BY DFT CALCULATION</b>		<b>65</b>
3.1	Introduction	65
3.2	Computational Chemistry Methods: <i>ab initio</i> and Density Functional Theory	65
3.2.1	Hartree-Fock Method	66
3.2.2	Density Functional Theory (DFT)	67
3.2.3	DFT Calculation for structures of TiO <sub>2</sub> and C-doped TiO <sub>2</sub>	69
3.3	Computational Method	72
3.4	Results and Discussion	75
3.4.1	Cluster models of Anatase	75
3.4.2	DFT Study of Anatase TiO <sub>2</sub>	77
3.4.2.1	Performance of the Theoretical Methods in the Calculation of the Band Gap Energy and Cohesive Energy of Anatase Cluster	77
3.4.2.2	Effect of Structure Distortion on the Band Gap Energy and Cohesive Energy of Anatase Cluster of TiO <sub>2</sub>	87
3.4.2.3	Effect of Oxygen Vacancy on the Band Gap Energy of Anatase TiO <sub>2</sub>	91
3.4.3	DFT Study of C-Doped Anatase TiO <sub>2</sub>	94
3.5	Summary	100
<b>CHAPTER 4 STRUCTURE-PHOTOCATALYTIC ACTIVITY RELATIONSHIP OF CARBON DOPED TITANIUM DIOXIDE USING FUZZY GRAPH</b>		<b>103</b>
4.1	Introduction	103
4.2	Fuzzy Logic	103
4.2.1	Fuzzy Graph	104
4.2.2	Fuzzy Inference System	105
4.3	Study on Structure-Photocatalytic Activity Relationship of C-doped TiO <sub>2</sub> using Combination of Fuzzy Graph and Fuzzy Inference System	106

4.4	Crisp Graph Representing Structure-Physicochemical Properties Relationship with Photocatalytic Activity of Styrene with Aqueous Hydrogen Peroxide	108
4.4.1	Surface Area	109
4.4.2	Crystallite Size	110
4.4.3	Porosity	110
4.4.4	Phase and Crystallinity	110
4.4.5	Electron-hole Recombination	111
4.4.6	Band Gap Energy and Sub-band Gap Energy	111
4.4.7	Carbon Defects	111
4.4.8	Structure Distortion and Oxygen Vacancy	112
4.5	Vertices and Links of the Network of 6 Variables	112
4.6	Development of Fuzzy Inference System Model	114
4.7	Fuzzy Graph Representing Relationship between Structural-Physicochemical Properties and Photocatalytic Activity	120
4.8	Summary of the Structure-Photocatalytic Activity Relationship of C-doped TiO <sub>2</sub> Photocatalyst	124
<b>CHAPTER 5</b>	<b>CONCLUSION AND RECOMMENDATIONS</b>	<b>125</b>
5.1	Conclusion	125
5.2	Recommendations	127
	<b>REFERENCES</b>	<b>129</b>
	<b>LIST OF PUBLICATIONS</b>	<b>175</b>

## LIST OF TABLES

TABLE NO.	TITLE	PAGE
Table 2.1	The reviews of structure-photocatalytic activity relationship of TiO <sub>2</sub> .	23
Table 2.2	List of the prepared samples with the corresponding code names.	26
Table 2.3	Elemental composition of Ti, O and C for TiO <sub>2</sub> samples	32
Table 2.4	Crystallite size and phase composition of C-doped TiO <sub>2</sub> .	36
Table 2.5	Surface area and pore size distribution of the samples calculated from BJH distribution	48
Table 2.6	Band gap energy of samples as calculated from optical absorption spectra.	51
Table 2.7	The atomic percentage of C 1s, O 1s and Ti 2p for all samples	58
Table 2.8	The atomic percent for each C peaks	59
Table 2.9	The summary of the physicochemical and electronic properties of CTAB-C/TiO <sub>2</sub> and C/TiO <sub>2</sub> at different calcination temperature, and the yield of products from the photocatalytic oxidation of styrene with hydrogen peroxide	64
Table 3.1	Summary of optimized lattice parameters, calculated band gaps and percent band gap error reported in previous works according to DFT approaches.	71
Table 3.2	Experimental parameters of TiO <sub>2</sub> (Anatase).	73
Table 3.3	Description of TiO <sub>2</sub> cluster	77
Table 3.4	Total energy, $E$ (a.u.), absolute value of total cohesive energy, $E_c$ (eV), absolute value of cohesive energy per atom, $E_c / atom$ (eV/atom), absolute value of cohesive energy per TiO <sub>2</sub> formula unit, $E_c / TiO_2$ (eV/TiO <sub>2</sub> ), theoretical band gap energy, $E_g$ (eV) and band gap error (%) for anatase, TiO <sub>2</sub> clusters calculated at HF and different DFT methods/6-311G(d).	79
Table 3.5	Total energy, $E$ (a.u.), absolute value of total cohesive energy, $E_c$ (eV), absolute value of cohesive energy per atom, $E_c / atom$ (eV/atom), theoretical band gap energy, $E_g$ (eV) and band gap energy error (%) calculated at	

	B2PLYP/6-311G(d) and B2PLYP/3-21G level of DFT for anatase TiO <sub>2</sub> cluster models.	84
Table 3.6	Mulliken charge transfer analysis of anatase Ti <sub>13</sub> O <sub>18</sub> cluster using different theoretical methods and basis set.	87
Table 3.7	Total energy, $E$ (a.u.), absolute value of total cohesive energy, $E_c$ (eV), absolute value of cohesive energy per atom, $E_c / atom$ (eV/atom) and theoretical band gap energy, $E_g$ (eV) at different value of structural distortion, $r$ (Å), for anatase Ti <sub>13</sub> O <sub>18</sub> cluster at B2PLYP/6-311G(d) level and Ti <sub>59</sub> O <sub>100</sub> cluster at B2PLYP/3-21G level of DFT.	88
Table 3.8	Total energies, $E$ (a.u.), absolute value of total cohesive energy, $E_c$ (eV), theoretical band gap energy, $E_g$ (eV), dipole moments (debye) for anatase Ti <sub>21</sub> O <sub>30</sub> cluster at different location of oxygen vacancy located at B2PLYP/6-311G(d) level of theory.	92
Table 3.9	Amount of C (at%), total energies, $E$ (a.u.), formation energies, $E_f$ (eV), absolute value of total cohesive energy, $E_c$ (eV), absolute value of cohesive energy per atom, $E_c / atom$ (eV/atom), theoretical band gap energy, $E_g$ (eV), dipole moments (debye) and net charges for C-doped anatase Ti <sub>21</sub> O <sub>30</sub> cluster at different amount of C (%) and location of C calculated at B2PLYP/6-311G(d) level of theory.	96
Table 4.1	Experimental data and predicted response of fuzzy logic model for photocatalytic activity under UV and visible light irradiations along with 6 independent variables of physicochemical properties.	118
Table 4.2	MSE, RMSE, ARE, AARE, SD and R <sup>2</sup> for photocatalytic activity under irradiations of UV and visible light from the fuzzy logic model.	120
Table 4.3	Sensitivity of each input parameter on photocatalytic oxidation of styrene under irradiations of UV and visible light.	121
Table 5.1	Amount of C (at%), total energies, $E$ (a.u.), formation energies, $E_f$ (eV), absolute value of total cohesive energy, $E_c$ (eV), absolute value of cohesive energy per atom, $E_c / atom$ (eV/atom), theoretical band gap energy, $E_g$ (eV), dipole moments (debye) and net charges (eV) for C-doped anatase Ti <sub>59</sub> O <sub>100</sub> cluster at different amount of C and location of C calculated at B2PLYP/3-21G level of theory.	167

## LIST OF FIGURES

FIGURE NO.	TITLE	PAGE
Figure 1.1	Schematic presentation of the research plan	4
Figure 2.1	Application of TiO <sub>2</sub> [6].	10
Figure 2.2	The tetragonal bulk unit cell of (a) anatase and (b) rutile dimension [40]. All structures have slightly distorted octahedral basic units, indicating the bond lengths with the angles of the octahedral Ti atoms.	13
Figure 2.3	Stacking of octahedral structures of TiO <sub>2</sub> (a) anatase, (b) rutile and (c) brookite [38].	13
Figure 2.4	Anatase TiO <sub>2</sub> molecular orbital diagram at different states of (a) atomic, (b) crystal field split, (c) final [41].	14
Figure 2.5	The spectrum of solar radiation [43].	15
Figure 2.6	Photoreaction of photocatalysts	18
Figure 2.7	The styrene reaction mechanism for benzaldehyde and styrene oxide production by porous C-coated TiO <sub>2</sub> [65,71].	20
Figure 2.8	XRD patterns of (a) commercial TiO <sub>2</sub> , and CTAB-C/TiO <sub>2</sub> at different calcination temperature of (b) 300, (c) 400, (d) 500, (e) 600 and (f) 700 °C.	34
Figure 2.9	XRD patterns of (a) commercial TiO <sub>2</sub> , and C/TiO <sub>2</sub> at different calcination temperature of (b) 300, (c) 400, (d) 500, (e) 600 and (f) 700 °C.	35
Figure 2.10	FTIR spectra for (a) commercial TiO <sub>2</sub> and the calcined CTAB-C/TiO <sub>2</sub> at temperatures of (b) 300, (c) 400, (d) 500, (e) 600, and (f) 700 °C. The inset to the figure is the zoomed-in peak for the stretching vibrations of C-O from 1500 – 1000 cm <sup>-1</sup> .	38
Figure 2.11	FTIR spectra for (a) commercial TiO <sub>2</sub> and the calcined C/TiO <sub>2</sub> temperatures of (b) 300, (c) 400, (d) 500, (e) 600, and (f) 700 °C. The inset to the figure is the zoomed-in peak for the stretching vibrations of C-O from 1500 – 1000 cm <sup>-1</sup> .	39
Figure 2.12	FTIR-ATR spectra for (a) commercial TiO <sub>2</sub> and the calcined CTAB-C/TiO <sub>2</sub> at temperatures of (b) 300, (c) 400, (d) 500, (e) 600, and (f) 700 °C.	40

Figure 2.13	FTIR-ATR spectra for (a) commercial TiO <sub>2</sub> and the calcined C/TiO <sub>2</sub> at temperatures of (b) 300, (c) 400, (d) 500, (e) 600, and (f) 700 °C.	41
Figure 2.14	FESEM images of (a) commercial TiO <sub>2</sub> , (b) CTAB-C/TiO <sub>2</sub> -300, and (c) CTAB-C/TiO <sub>2</sub> -700 (d) C/TiO <sub>2</sub> -300 and (e) C/TiO <sub>2</sub> -700	43
Figure 2.15	N <sub>2</sub> adsorption-desorption isotherms of (a) commercial TiO <sub>2</sub> and CTAB-C/TiO <sub>2</sub> samples at different calcination temperature of (b) 300, (c) 400, (d) 500, (e) 600, and (f) 700 °C.	44
Figure 2.16	N <sub>2</sub> adsorption-desorption isotherms of (a) commercial TiO <sub>2</sub> and C/TiO <sub>2</sub> samples at different calcination temperature of (b) 300, (c) 400, (d) 500, (e) 600, and (f) 700 °C	45
Figure 2.17	Pore size distribution curve of the isotherm of (a) commercial TiO <sub>2</sub> and CTAB-C/TiO <sub>2</sub> samples at different calcination temperature (b) 300, (c) 400, (d) 500, (e) 600, and (f) 700 °C.	46
Figure 2.18	Pore size distribution curve of the isotherm of (a) commercial TiO <sub>2</sub> and C/TiO <sub>2</sub> samples at different calcination temperature (b) 300, (c) 400, (d) 500, (e) 600, and (f) 700 °C.	47
Figure 2.19	UV-Vis DR spectra of (a) commercial TiO <sub>2</sub> , (b) CTAB-C/TiO <sub>2</sub> -300, (c) CTAB-C/TiO <sub>2</sub> -400, (d) CTAB-C/TiO <sub>2</sub> -500, (e) CTAB-C/TiO <sub>2</sub> -600, and (f) CTAB-C/TiO <sub>2</sub> -700.	49
Figure 2.20	UV-Vis DR spectra of (a) commercial TiO <sub>2</sub> , (b) C/TiO <sub>2</sub> -300, (c) C/TiO <sub>2</sub> -400, (d) C/TiO <sub>2</sub> -500, (e) C/TiO <sub>2</sub> -600 and (f) C/TiO <sub>2</sub> -700.	50
Figure 2.21	Photoluminescence spectra of (a) CTAB-C/TiO <sub>2</sub> and (b) C/TiO <sub>2</sub> samples at different calcination temperature 300 to 700 °C.	52
Figure 2.22	XPS survey spectra of (a) commercial TiO <sub>2</sub> , (b) CTAB-C/TiO <sub>2</sub> -500, (c) CTAB-C/TiO <sub>2</sub> -700 (d) C/TiO <sub>2</sub> -500 and (e) C/TiO <sub>2</sub> -700,	54
Figure 2.23	The binding energy of Ti2p of (a) commercial TiO <sub>2</sub> , (b) CTAB-C/TiO <sub>2</sub> -500, (c) CTAB-C/TiO <sub>2</sub> -700, (d) C/TiO <sub>2</sub> -500 and (e) C/TiO <sub>2</sub> -700,	55
Figure 2.24	The binding energy of O1s of (a) commercial TiO <sub>2</sub> , (b) CTAB-C/TiO <sub>2</sub> -500, (c) CTAB-C/TiO <sub>2</sub> -700, (d) C/TiO <sub>2</sub> -500 and (e) C/TiO <sub>2</sub> -700,	56

Figure 2.25	The binding energy of C1s of (a) commercial TiO <sub>2</sub> (b) CTAB-C/TiO <sub>2</sub> -500, (c) CTAB-C/TiO <sub>2</sub> -700 (d) C/TiO <sub>2</sub> -500 and (e) C/TiO <sub>2</sub> -700	57
Figure 2.26	Concentration of products after the reaction of 5 mmol of styrene with hydrogen peroxide under the irradiations of (a) UV and, (b) visible light for commercial TiO <sub>2</sub> and prepared C-doped TiO <sub>2</sub> at room temperature for 24 h. The exact styrene conversion and yield of benzaldehyde and styrene oxide is tabulated in Appendix A.	60
Figure 3.1	Cluster models of anatase TiO <sub>2</sub> (a) Ti <sub>13</sub> O <sub>18</sub> , (b) Ti <sub>21</sub> O <sub>30</sub> , (c) Ti <sub>29</sub> O <sub>42</sub> , (d) Ti <sub>34</sub> O <sub>50</sub> , (e) Ti <sub>59</sub> O <sub>100</sub> , (f) Ti <sub>65</sub> O <sub>98</sub> , and (g) Ti <sub>163</sub> O <sub>294</sub> (yellow spheres and red spheres are Ti and O atoms, respectively).	76
Figure 3.2	Band gap energy of anatase TiO <sub>2</sub> cluster versus HF, MP2 and various DFT theoretical methods with 6-311G(d) basis set.	82
Figure 3.3	Band gap energy versus anatase cluster sizes at 6-311G(d) and 3-21G basis set.	85
Figure 3.4	Partial density of states (PDOS) for (a) Ti <sub>21</sub> O <sub>30</sub> cluster calculated at B2PLYP/6-311G(d) and (b) Ti <sub>59</sub> O <sub>100</sub> cluster calculated at B2PLYP/3-21G.	86
Figure 3.5	Variation of the absolute energy versus distortion of Ti <sub>13</sub> O <sub>18</sub> cluster at B2PLYP/6-311G(d).	89
Figure 3.6	Calculated band gap energy versus distortion, r for Ti <sub>13</sub> O <sub>18</sub> cluster at B2PLYP/6-311G(d), B2PLYP/3-21G and Ti <sub>59</sub> O <sub>100</sub> cluster at B2PLYP/3-21G.	90
Figure 3.7	Partial density of states (PDOS) for (a) Ti <sub>59</sub> O <sub>100</sub> clusters and (b) Ti <sub>59</sub> O <sub>100</sub> clusters distort at -0.06 Å calculated at B2PLYP/3-21G.	91
Figure 3.8	Location of the oxygen vacancy in Ti <sub>21</sub> O <sub>30</sub> .	92
Figure 3.9	PDOS for (a) Ti <sub>21</sub> O <sub>30</sub> cluster, oxygen vacancy at (b) O <sub>1</sub> , and (c) O <sub>2</sub> in Ti <sub>21</sub> O <sub>30</sub> clusters at B2PLYP/6-311G(d).	94
Figure 3.10	Models for the anatase C-doping anatase Ti <sub>21</sub> O <sub>30</sub> at different substitutional and interstitial position (The yellow and red spheres represent the Ti and O atoms, respectively. The numbered red spheres (1-3) and yellow spheres (4-5) denote the positions of O and Ti substituted by the C dopants, respectively and the violet numbered spheres (6-7) notify the interstitial doping positions).	95
Figure 3.11	Calculated TDOS and PDOS for (a) pure anatase Ti <sub>21</sub> O <sub>30</sub> ; and C-doped Ti <sub>21</sub> O <sub>30</sub> at different position of (b) C@O <sub>1</sub> (c)	

	C@O <sub>2</sub> (d) C@O <sub>3</sub> (e) C@O <sub>1</sub> O <sub>2</sub> (f) C@O <sub>1</sub> O <sub>3</sub> (g) O <sub>1</sub> O <sub>2</sub> O <sub>3</sub> (h) Ti <sub>4</sub> (i) Ti <sub>5</sub> (j) Ti <sub>4</sub> Ti <sub>5</sub> (k) C@in <sub>6</sub> (l) C@in <sub>7</sub> (m) C@in <sub>6</sub> in <sub>7</sub>	99
Figure 4.1	Fuzzy Inference System [16].	105
Figure 4.2	Flow chart for the structure-photocatalytic activity relationship of C-doped TiO <sub>2</sub> using fuzzy logic	107
Figure 4.3	Graph G showing the correlation between input-output variables of the relationship between structural and physicochemical properties and photocatalytic activities (straight line is a relationship based on experimental study while dotted line is a relationship based on DFT study)	109
Figure 4.4	Graph G showing the correlation between input-output variables of the relationship between structural and physicochemical properties and photocatalytic activities. Straight line is a relationship based on experimental study while dotted line is a relationship based on DFT study.	114
Figure 4.5	Fuzzy membership functions of the input variables (SA, PH, e-h and %C) and output variables (PCA of styrene under UV and visible light irradiations).	117
Figure 4.6	Comparison between the predicted data using fuzzy inference model and the experimental data of styrene conversion (%) efficiency under (a) UV and (b) visible light irradiations.	119
Figure 4.7	Fuzzy graph showing the correlation between input-output variables of the relationship between structural and physicochemical properties and photocatalytic activity of styrene under (a) UV light and (b) visible light irradiations. Red line is a fuzzy connectivity while black line is crisp connectivity.	122
Figure 5.1	Models for the anatase C-doping anatase Ti <sub>59</sub> O <sub>100</sub> at different substitutional and interstitial position (The yellow and red spheres represent the Ti and O atoms, respectively. The numbered red spheres (1-4) and yellow spheres (5-7) denote the positions of O and Ti substituted by the C dopants, respectively and the violet numbered spheres (8-9) notify the interstitial doping positions).	166
Figure 5.2	Calculated TDOS and PDOS for (a) pure anatase Ti <sub>59</sub> O <sub>100</sub> ; C mono-doping of Ti <sub>59</sub> O <sub>100</sub> anatase at (b) C@O <sub>1</sub> , (c) C@Ti <sub>4</sub> , (d) C@in <sub>6</sub> , (e) C@O <sub>1</sub> O <sub>2</sub> , (f) C@Ti <sub>4</sub> Ti <sub>5</sub> (g) C@in <sub>6</sub> in <sub>7</sub> and (h) C@O <sub>1</sub> O <sub>2</sub> O <sub>3</sub> .	169



## LIST OF ABBREVIATIONS

$\lambda$	-	Wavelength
$2\theta$	-	Bragg angle
Å	-	Angstrom
a.u.	-	Arbitrary unit
ARE	-	Average relative error
AARE	-	Absolute average error
ANA	-	Anatase
BET	-	Brunauer-Emmet-Teller
BG	-	Band gap energy
BJH	-	Barret-Joyner-Halenda
%C	-	Amount of carbon in percent
C	-	Carbon
C/TiO <sub>2</sub>	-	C-doped TiO <sub>2</sub> samples without addition of CTAB
CASTEP	-	Cambridge serial total energy package
CB	-	Covalent band
CdS	-	Cadmium sulfide
CTAB	-	Cetyltrimethylammonium bromide
CTAB-C/TiO <sub>2</sub>	-	C-doped TiO <sub>2</sub> samples with addition of CTAB
D	-	Debye
DFT	-	Density functional theory
EDX	-	Energy dispersive X-ray spectroscopy
$E$		Energy
$E_c$	-	Cohesive energy
$E_f$	-	Formation energy
$E_g$	-	Band gap energy
e <sup>-</sup>	-	Electron
e-h	-	Amount of electron-hole recombine
FESEM	-	Field emission scanning electron microscope
FTIR	-	Fourier transform infrared
GC	-	Gas chromatography

GGA	-	Gradient approximations
$h^+$	-	Positive hole
H <sub>2</sub> O <sub>2</sub>	-	Hydrogen peroxide
HF	-	Hartree fock
m	-	Meters
min	-	Minute(s)
mL	-	Milliliter
MP2	-	2 <sup>nd</sup> order Moller-Plesset perturbation theory
MSE	-	Mean squared normalized error
nm	-	Nanometers
PBE	-	Perdew-Burke-Ernzerhof
PCA	-	Photocatalytic activity
PDOS	-	Partial density of states
PH	-	Phase
PL	-	Photoluminescence
RMSE	-	Root mean squared error
RUT	-	Rutile
SA	-	Surface area
SBG	-	Sub-band gap energy
SD	-	Standard deviation
TDOS	-	Total density of states
TEM	-	Transmission electron microscope
TGA	-	Thermogravimetric analysis
TiO <sub>2</sub>	-	Titanium dioxide
UV-Vis	-	Ultraviolet-visible
UV-Vis DR	-	UV-Visible diffuse reflectance
VASP	-	The Vienna <i>ab initio</i> simulation package
VB	-	Valence band
XRD	-	X-ray diffraction
ZnO	-	Zinc oxide

## LIST OF APPENDICES

APPENDIX	TITLE	PAGE
Appendix A	Styrene Conversion and Yield of Products for Photocatalytic Oxidation of Styrene	147
Appendix B	Calibration Curve of Products for Photocatalytic Oxidation of Styrene	148
Appendix C	Qualitative / Crisp Scale for Phase Crystallinity and Amount of Electron-Hole Recombine	149
Appendix C	Band gap evaluation for linear dependence of $(F(R_{\infty}).h\nu)^{1/2}$ versus photon energy	150
Appendix D	Thermogravimetric and Different Scanning Calorimeter Analysis	151
Appendix E	Fractional and Cartesian Coordinates for Primitive Unit Cell of Anatase ( $Ti_{13}O_{18}$ )	152
Appendix F	Gaussian 09 Input Files	153
Appendix G	Gaussian 09 Output Files	154
Appendix H	PDOS for C-doping in $Ti_{21}O_{30}$ cluster	162
Appendix I	C-doping for $Ti_{59}O_{100}$ cluster	166
Appendix J	Rules of Fuzzy Inference System	170
Appendix K	Details Equation for MSE, RMSE, ARE, AARE, SD and $R^2$	172
Appendix L	Three Dimensional Surfaces of Fuzzy Model Rules	173

# CHAPTER 1

## INTRODUCTION

### 1.1 Background of Study

Major concerns on the rising number of environmental problems have resulted in compulsive development of environmental purification methods. This fundamental advanced environmental solution has drawn attention and gained importance due to its full potential in bringing a significant change in human life. Therefore, a great deal of research efforts have been done on photocatalysis in various areas such as degradation of organic and inorganic pollutants, hydrogen production and organic synthesis [1].

Titanium dioxide,  $\text{TiO}_2$  or titania is the most widely studied material due to its superior performance since 1972 when Fujishima and Honda reported water decomposition using  $\text{TiO}_2$  electrode as a potential semiconductor photocatalytic material [2,3].  $\text{TiO}_2$  is known as an outstanding and promising material in paints pigments, degradation of water pollutants, electrochromic displays, electrochemical electrodes, capacitors, lithium-ion batteries, sensors and catalysts' support [4–6].

$\text{TiO}_2$  is a commonly used photocatalytic material due to its rather low material cost, high chemical stability, high specific surface area and nontoxicity [7–9]. It is generally believed that a relationship exists between  $\text{TiO}_2$  photocatalyst's physicochemical properties and photocatalytic activity. However, the discussion on the relationship between the physicochemical properties of  $\text{TiO}_2$  and its photocatalytic activity is limited, and there seems to be no comprehensive approach or tool to discuss this relationship. The discussion has been restricted to several samples synthesized in a similar manner or a small number of commercial samples [10]. Ohtani [11,12] who has made a significant contribution to heterogeneous photocatalysis for more than 30 years and has published over 200 original and review papers on photocatalysis, also

remains frustrated with the fact that the structure-photocatalytic activity relationship of photocatalyst has not yet been clarified [11].

Furthermore, the main dominant factor has not been clearly investigated by a comprehensive method. Previous study done by Muniandy [13] reported that the surface area was the main factor which enhanced the photocatalytic activity of TiO<sub>2</sub> photocatalyst. However, previous works [14,15] also found the surface area may be a requirement but cannot be the decisive factor for the enhanced photocatalytic activity. It was found that surface properties (i.e. acidity of the surface and hydroxyl groups content) and synergistic effect of C-doping at interstitial position and surface carbonaceous species, were the main factors that can improve the performance of TiO<sub>2</sub> as a photocatalyst.

Prieto-Mahaney and coworkers [10] are among the sole researchers that studied the comprehensive relationship between the structural and physical properties with the photocatalytic activity of TiO<sub>2</sub> powders using mathematical methods. Statistical multivariable analyses were used with the aim of obtaining the relationship of six properties of 35 commercially available TiO<sub>2</sub> samples in Japan, with five photocatalytic reactions. From the statistical multivariable analyses, it was found that the photocatalytic activities strongly depended on the properties of the TiO<sub>2</sub> powders. However, this method required higher number of samples, which are a major limitation on determining the structure-photocatalytic activity of TiO<sub>2</sub>.

Besides that, some of the properties are imprecise or incomplete data have been given in the series of samples [16]. The data also cannot be generalized and analysed using binary logic (1 or 0 / true or false) that are precise and in discrete terms. Therefore, the computational intelligence technique is desperately required that accounts for all complexities and variations of data in investigating the structure-photocatalytic activity relationship of TiO<sub>2</sub> photocatalyst. Recently, the use of computational techniques for various applications, including modeling and problem solving, has attracted considerable interest between researchers, primarily in the science and engineering area. Fuzzy logic is the nearest solution to complex problems which has the potential of combining human thought and experience into computer-assisted decision making.

Zadeh introduced fuzzy logic, which takes into account the complexity of the real world and the uncertainty that everything cannot have absolute values and follow a linear function [17]. Fuzzy logic deal with vague, indecisive ideas and subjective information which depending on “degrees of truth” (0 to 1) instead of the usual “true or false” (1 or 0). It is also possible to calculate exactly the qualitative and quantitative variables with different amounts and meanings[18]. To the best of our knowledge, no study has been reported in the literature on the relationship between TiO<sub>2</sub> photocatalyst’s physicochemical properties and its photocatalytic activity using fuzzy logic.

Fuzzy graph is another focus on the implementation of fuzzy theory in its relation to the theory of graphs. Fuzzy graph in the form of a graph describes the relationship between variables, which accurately shows the relationship degree between variables. Therefore, in this study, fuzzy graph in the form of graph is applied to clarify the structure-photocatalytic activity relationship of TiO<sub>2</sub> photocatalyst. Imagine combining the physicochemical properties and photocatalytic activity of all data in current literature to clarify the structure-photocatalytic activity relationship of TiO<sub>2</sub> photocatalyst between them using fuzzy logic.

Carbon doped TiO<sub>2</sub> (C-doped TiO<sub>2</sub>) was chosen as the photocatalyst model in explaining the structure-photocatalytic relationship of TiO<sub>2</sub>. The addition of carbon, C to TiO<sub>2</sub> semiconductor’s lattice are believed to one of the suitable methods to modify TiO<sub>2</sub> to enhance its photocatalytic performance. Furthermore, the preparation of TiO<sub>2</sub> usually contains C impurity, which is difficult to remove, and this C impurity significantly affects the TiO<sub>2</sub> photocatalytic activity. The modification of TiO<sub>2</sub> with carbon can generally change the structure, physicochemical and electronic properties of TiO<sub>2</sub> which enhance its photocatalytic performance by facilitating faster transport to the active sites on TiO<sub>2</sub>’s surface, narrowing the band gap energy, extending the light absorption to visible range and suppressing the rate of electron-hole recombination [19].

However, in order to clarify the structure-photocatalytic activity relationship of TiO<sub>2</sub> photocatalyst, the experimental approach is not enough. A theoretical

approach by DFT calculation is also necessary to be carried out to determine the electronic structure of C-doped TiO<sub>2</sub> photocatalyst. DFT is a computational method that is used to calculate the properties and electronic band structures of molecules using the results of the theoretical quantum chemistry. In this study, the combination of experimental work, DFT calculation and fuzzy graph may well explain the relationship between the C-doped TiO<sub>2</sub> physicochemical properties with its photocatalytic activity. The schematic presentation of the research plan is represented in Figure 1.1.

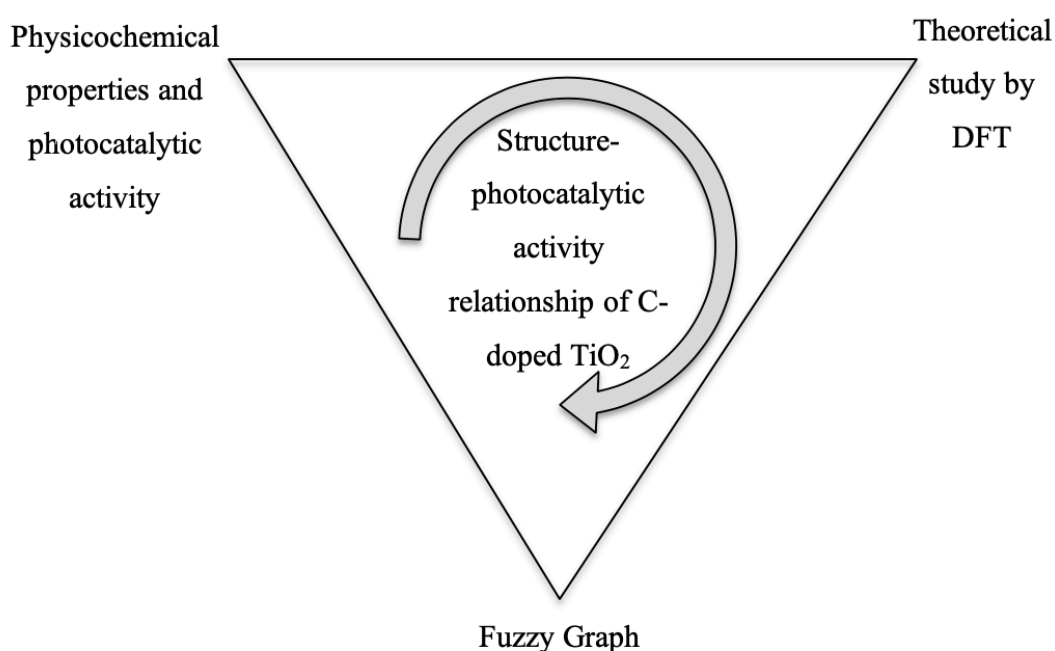


Figure 1.1 Schematic presentation of the research plan

## 1.2 Problem Statement

TiO<sub>2</sub> photocatalyst has gained significant attention as one of the most promising materials in the removal of various organic pollutants, such as organic dyes and phenolic compounds. It is known that photocatalytic activity is correlated with the structural and physicochemical properties of TiO<sub>2</sub>. However, there has been no clear explanation on the relationship between physicochemical properties and

photocatalytic reactions. In this research, to solve this problem, a new approach has been proposed to evaluate the structure-photocatalytic activity relationship with the aim to better understand the dominant properties in determining the photocatalytic activities of C-doped TiO<sub>2</sub>. The dominant properties found in the fuzzy graph can be used as a future guideline to synthesize the photocatalyst with high photocatalytic activity. Photooxidation of styrene has been used as the model of organic pollutant reaction due to the oxidation of styrene are importance for academics and industry, particularly in the production of fine chemicals including benzaldehyde. Fuzzy logic graph with the combination of fuzzy inference system modelling has been used as a new approach in determining the dominant factor for the structure-photocatalytic activity relationship of C-doped TiO<sub>2</sub>. Characterization results from experimental study were used in the fuzzy logic graph and the electronic structure were discussed with the theoretical calculations of C-doped TiO<sub>2</sub> using DFT. The C-doping, structure distortions and oxygen vacancy may affect electronic structure of anatase; that is why in this study further investigation of different C doping positions, and location of C, was necessary.

### **1.3 Objectives of Study**

Several objectives were set to study the structure-photocatalytic activity relationship of C-doped TiO<sub>2</sub> as follows:

- (a) To investigate the physicochemical properties of the prepared C-doped TiO<sub>2</sub> photocatalysts at different calcination temperature and their photocatalytic activity of styrene under UV and visible light irradiation.
- (b) To investigate the effect of C doping, structure distortion and oxygen vacancy on the band gap energy of anatase TiO<sub>2</sub> by DFT calculation
- (c) To clarify the structure-photocatalytic activity relationship of C-doped TiO<sub>2</sub> and the dominant properties that determine the photocatalytic activities of C-doped TiO<sub>2</sub> samples using fuzzy logic graph from experimental work and DFT calculation.



## 1.4 Scope of Study

This study demonstrated the combination of photocatalytic experiment, DFT and fuzzy logic graph analysis, can be used to clarify the structure-photocatalytic activity relationship in TiO<sub>2</sub> photocatalytic systems. In order to accomplish the research's objectives, the scope of the study is designated into three parts, which are the preparation of C-doped TiO<sub>2</sub> and its photocatalytic activity, theoretical study by DFT and fuzzy logic graph .

This study focussed on the preparation of anatase TiO<sub>2</sub> and C-doped anatase TiO<sub>2</sub> using the sol-gel process, calcined at different temperature of 300 to 700 °C. The synthesized materials were characterized by X-ray diffraction (XRD), Fourier transform infrared spectroscopy (FTIR), energy dispersive X-ray spectroscopy (EDX), field emission electron microscopy (FE-SEM), N<sub>2</sub> adsorption-desorption, UV-Visible diffuse reflectance (UV-Vis DR) spectroscopy, photoluminescence (PL) spectroscopy and X-Ray photoelectron spectroscopy (XPS). The photocatalytic activity of C-doped TiO<sub>2</sub> was evaluated in the photocatalytic oxidation of styrene, as the model reaction for organic pollutants under irradiations of UV and visible light.

DFT theoretical calculation was performed using Gaussian 09 to study the electronic properties of anatase TiO<sub>2</sub> and C-doped anatase TiO<sub>2</sub>. The scope of the DFT study were limited to only the anatase structure of TiO<sub>2</sub>. The performance of HF and five popular exchange-correlation functionals of DFT including hybrid (B3LYP, B3PW91, PBE1PBE or known as PBE0 and PBEh1PBE), double-hybrid functional (B2PLYP) and MP2 that is available in Gaussian 09 package was investigated in predicting band gap energy. In addition, the structure distortion and effect of C at different amount of C and location of C on the band gap energy of TiO<sub>2</sub> were studied using DFT calculation. The total density of states (TDOS) and partial density of states (PDOS) for C-doped anatase TiO<sub>2</sub> are plotted to further investigates the effect of C on the band gap energy and sub-band gap energy of anatase.

The combination of fuzzy logic graph and fuzzy inference system was used to study the structure-photocatalytic activity relationship of C-doped TiO<sub>2</sub>. Fuzzy

inference system model was developed by MATLAB software. A sensitivity analysis was carried out from developed fuzzy inference system model to obtain the membership value that represents the dominant properties that determine the photocatalytic activities of C-doped TiO<sub>2</sub> under irradiations of UV and visible light.

## 1.5 Significance of Study

This research provides an understanding on the structure-photocatalytic activity relationship and the dominant properties that determine the photocatalytic activities of C-doped TiO<sub>2</sub> photocatalytic system. Fuzzy logic graph with the combination of fuzzy inference system modelling has been proposed as a new approach to clarify the structure-photocatalytic activity relationship with the aim to better understand the dominant properties in determining the photocatalytic activities of C-doped TiO<sub>2</sub> supported with DFT calculation. The combination of photocatalytic experiment, DFT, and fuzzy logic graph analysis can be used to clarify the structure-photocatalytic activity relationship in TiO<sub>2</sub> photocatalytic systems. DFT explained the effect of structural distortion, oxygen vacancy, C-doped at different location and amount of C on the electronic structure of anatase TiO<sub>2</sub>. From the DFT study, double hybrid functional B2PLYP employing 6-311G(d) has been proposed as the accurate exchange-functional methods in predicting the TiO<sub>2</sub> band gap energy compared to the previous studies such as B3LYP, B3PW91, PBE1PBE, and PBEh1PBE. Furthermore, the dominant properties found in the fuzzy graph can be used as a future guideline to synthesize the photocatalyst with high photocatalytic activity.

## 1.6 Research Outline

This research was conducted in three parts. The first part, discussed in **Chapter 2**, is the preparation of C-doped TiO<sub>2</sub> using a simple sol-gel method. Various instruments were used to study the physicochemical properties of prepared C-doped TiO<sub>2</sub> photocatalyst. Five physicochemical properties of C-doped TiO<sub>2</sub> samples were analyzed in detail, including the crystal structure and crystallinity, functional groups,

chemical composition, morphology structure, surface area, porosity, and band gaps. Besides, to study the photocatalytic activity of C-doped TiO<sub>2</sub> samples, the photooxidation of styrene with aqueous hydrogen peroxide was tested as the model of organic pollutant reaction under UV and visible light irradiations.

The second part in **Chapter 3** discusses the electronic structure of C-doped TiO<sub>2</sub> by DFT calculation. For this section, the performance of the theoretical DFT methods in determining the anatase cluster's band gap energy was investigated to find the accurate methods for predicting TiO<sub>2</sub>'s band gap energy using Gaussian 09. Furthermore, the effect of structural distortion, oxygen vacancy, C-doped TiO<sub>2</sub> on the anatase TiO<sub>2</sub> band gap energy will be clarified.

The last part of the research in **Chapter 4**, involves the structure-photocatalytic activity relationship of C-doped TiO<sub>2</sub> samples and the dominant properties that determine the photocatalytic activities of the C-doped TiO<sub>2</sub> photocatalytic system using the fuzzy logic graph.

## REFERENCES

- [1] Lazar M.A., Varghese S. and Nair S.S. Photocatalytic Water Treatment by Titanium Dioxide: Recent Updates. *Catalysts*. 2012. 2: 572–601.
- [2] Paulauskas I.E., Modeshia D.R., Ali T.T., El-Mossalamy E.H., Obaid A.Y., Basahel S.N., Al-Ghamdi A.A. and Sartain F.K. Photocatalytic activity of doped and undoped titanium dioxide nanoparticles synthesised by flame spray pyrolysis. *Platinum Metals Review*. 2013. 57(1): 32–43.
- [3] Taga Y. Titanium oxide based visible light photocatalysts: Materials design and applications. *Thin Solid Films*. 2009. 517(10): 3167–72.
- [4] Abdullah A.M., Al-Thani N.J., Tawbi K. and Al-Kandari H. Carbon/Nitrogen-doped TiO<sub>2</sub>: New synthesis route, characterization and application for phenol degradation. *Arabian Journal of Chemistry*. 2015. 9(2): 229–37.
- [5] Wong C.L., Tan Y.N. and Mohamed A.R. A review on the formation of titania nanotube photocatalysts by hydrothermal treatment. *Journal of Environmental Management*. 2011. 92(7): 1669–80.
- [6] Nakata K. and Fujishima A. TiO<sub>2</sub> photocatalysis: Design and applications. *Journal of Photochemistry and Photobiology C: Photochemistry Reviews*. 2012. 13(3): 169–89.
- [7] Ganesan N.M., Muthukumarasamy N., Balasundaraprabhu R. and Senthil T.S. Importance of carbon (prepared from *Azadirachta indica*) for photocatalytic applications. *Optik*. 2015. 126(22): 3317–20.
- [8] Lavand A.B. and Malghe Y.S. Nano sized C doped TiO<sub>2</sub> as a visible light photocatalyst for the degradation of 2,4,6-trichlorophenol. *Advanced Materials Letters*. 2015. 6(8): 695–700.
- [9] Kumar N., Hazarika S.N., Limbu S., Boruah R., Deb P., Namsa N.D. and Das S.K. Hydrothermal synthesis of anatase titanium dioxide mesoporous microspheres and their antimicrobial activity. *Microporous and Mesoporous Materials*. 2015. 213: 181–7.
- [10] Prieto-Mahaney O.-O., Murakami N., Abe R. and Ohtani B. Correlation between photocatalytic activities and structural and physical properties of titanium (IV) oxide powders. *Chemistry Letters*. 2009. 38(3): 7–8.

- [11] Ohtani B. Photocatalysis A to Z — What we know and what we do not know in a scientific sense. *Journal of Photochemistry & Photobiology, C: Photochemistry Reviews*. 2011. 11(4): 157–78.
- [12] Ohtani B. Hidden but possibly fatal misconceptions in photocatalysis studies: A short critical review. *Catalysts*. 2016. 6(192): 1–6.
- [13] Muniandy L., Adam F., Mohamed A.R., Ng E.P. and Rahman N.R.A. Carbon modified anatase TiO<sub>2</sub> for the rapid photo degradation of methylene blue: A comparative study. *Surfaces and Interfaces*. 2016. 5: 19–29.
- [14] Kavitha R. and Devi L.G. Synergistic effect between carbon dopant in titania lattice and surface carbonaceous species for enhancing the visible light photocatalysis. *Journal of Environmental Chemical Engineering*. 2014. 2(2): 857–67.
- [15] Vorontsov A. V., Kabachkov E.N., Balikhin I.L., Kurkin E.N., Troitskii V.N. and Smirniotis P.G. Correlation of surface area with photocatalytic activity of TiO<sub>2</sub>. *Journal of Advanced Technologies*. 2018. 21(1).
- [16] Javadian H., Ghasemi M., Maria A., Mostafa S., Asl H. and Masomi M. Fuzzy logic modeling of Pb(II) sorption onto mesoporous NiO/ZnCl<sub>2</sub>-Rosa Canina-L seeds activated carbon nanocomposite prepared by ultrasound-assisted coprecipitation technique. *Ultrasonics - Sonochemistry*. 2018. 40: 748–62.
- [17] Godil S.S., Shamim M.S., Enam S.A. and Qidwai U. Fuzzy logic : A “simple” solution for complexities in neurosciences? *Surgical Neurology International*. 2011. 2(24).
- [18] Javadian H., Asadollahpour S., Maria A., Ghasemi M., Mostafa S., Asl H. and Masomi M. Using fuzzy inference system to predict Pb(II) removal from aqueous solutions by magnetic Fe<sub>3</sub>O<sub>4</sub>/H<sub>2</sub>SO<sub>4</sub>-activated Myrtus Communis leaves carbon nanocomposite. *Journal of the Taiwan Institute of Chemical Engineers*. 2018. 91: 186–99.
- [19] Palanivelu K., Im J.S. and Young-Seak L. Carbon doping of TiO<sub>2</sub> for visible light photo catalysis-A review. *Carbon Science*. 2007. 8(3): 214–24.
- [20] Ameta R. and Ameta S.C. Photocatalysis: Principles and Applications. 2017. 1–324 p.
- [21] Tang W., Chen X., Xia J., Gong J. and Zeng X. Preparation of an Fe-doped visible-light-response TiO<sub>2</sub> film electrode and its photoelectrocatalytic activity. *Materials Science and Engineering B: Solid-State Materials for Advanced*

- Technology*. 2014. 187: 39–45.
- [22] Ohtani B. Revisiting the fundamental physical chemistry in heterogeneous photocatalysis : its thermodynamics and kinetics. *Physical chemistry chemical physics : PCCP*. 2014. 16: 1788–97.
- [23] Dong F., Xiong T., Sun Y., Lu L., Zhang Y., Zhang H., Huang H., Zhou Y. and Wu Z. Exploring the photocatalysis mechanism on insulators. *Applied Catalysis B: Environmental*. 2017. 219: 450–8.
- [24] Bréchnignac C., Houdy P. and Lahmani M. *Nanomaterials and Nanochemistry*. 2008. 747 p.
- [25] Shah E., Vaghasiya J. V., Soni S.S., Panchal C.J., Suryavanshi P.S., Chavda M. and Soni H.P. Ni doped ZnS nanoparticles as photocatalyst: Can mixed phase be optimized for better performance? *Journal of Environmental Chemical Engineering*. 2016. 4(4): 4708–18.
- [26] Hoffmann M.R., Martin S.T., Choi W. and Bahnemann D.W. Environmental applications of semiconductor photocatalysis. *Chemical Reviews*. 1995. 95: 69–96.
- [27] Lin Z., Yin M. and Wang M. Multifunctional photocatalytic materials for energy. 2018. 333 p.
- [28] Carp O., Huisman C.L. and Reller A. Photoinduced reactivity of titanium dioxide. 2004. 32: 33–177.
- [29] Li Puma G., Bono A. and Collin J.G. Preparation of titanium dioxide photocatalyst loaded onto activated carbon support using chemical vapor deposition: A review paper. *Journal of Hazardous Materials*. 2008. 157(2–3): 209–19.
- [30] Graciani J., Ortega Y. and Sanz J.F. Carbon doping of the TiO<sub>2</sub> (110) rutile surface. A theoretical study based on DFT. *Chem Mater*. 2009. 21: 1431–8.
- [31] Lan Y., Lu Y. and Ren Z. Mini review on photocatalysis of titanium dioxide nanoparticles and their solar applications. *Nano Energy*. 2013. 2(5): 1031–45.
- [32] Yu C., Zhou W., Yu J.C., Liu H. and Wei L. Design and fabrication of heterojunction photocatalysts for energy conversion and pollutant degradation. *Chinese Journal of Catalysis*. 2014. 35(10): 1609–18.
- [33] Liu J., Zhang Q., Yang J., Ma H., Tade M.O., Wang S. and Liu J. Facile synthesis of carbon-doped mesoporous anatase TiO<sub>2</sub> for the enhanced visible-light driven photocatalysis. *Chem Commun*. 2014. 50: 13971–4.

- [34] Yang D., Liu H., Zheng Z., Yuan Y., Zhao J.C., Waclawik E.R., Ke X. and Zhu H. An efficient photocatalyst structure: TiO<sub>2</sub>(B) nanofibers with a shell of anatase nanocrystals. *Journal of the American Chemical Society*. 2009. 131(10): 17885–93.
- [35] He Z., Que W., Chen J., He Y. and Wang G. Surface chemical analysis on the carbon-doped mesoporous TiO<sub>2</sub> photocatalysts after post-thermal treatment: XPS and FTIR characterization. *Journal of Physical and Chemistry of Solids*. 2013. 74(7): 924–8.
- [36] Scanlon D.O., Dunnill C.W., Buckeridge J., Shevlin S.A., Logsdail A.J., Woodley S.M., Catlow C.R.A., Powell M.J., Palgrave R.G., Parkin I.P., Watson G.W., Keal T.W., Sherwood P., Walsh A. and Sokol A.A. Band alignment of rutile and anatase TiO<sub>2</sub>. *Nature Materials*. 2013. 12(9): 798–801.
- [37] Ortiz A.L., Zaragoza M.M., Gutierrez J.S., Paula M.M. da S. and Collins-Martinez V. Silver oxidation state effect on the photocatalytic properties of Ag doped TiO<sub>2</sub> for hydrogen production under visible light. *International Journal of Hydrogen Energy*. 2015. : 1–8.
- [38] Pelaez M., Nolan N.T., Pillai S.C., Seery M.K., Falaras P., Kontos A.G., Dunlop P.S.M., Hamilton J.W.J., Byrne J.A., O’Shea K., Entezari M.H. and Dionysiou D.D. A review on the visible light active titanium dioxide photocatalysts for environmental applications. *Applied Catalysis B: Environmental*. 2012. 125: 331–49.
- [39] Atanelov J., Gruber C. and Mohn P. The electronic and magnetic structure of p-element (C,N) doped rutile-TiO<sub>2</sub>; a hybrid DFT study. *Computational Materials Science*. 2015. 98: 42–50.
- [40] Diebold U. The surface science of titanium dioxide. *Surface Science Reports*. 2003. 48(5–8): 53–229.
- [41] Peng H., Li J., Li S.-S. and Xia J.-B. First-principles study of the electronic structures and magnetic properties of 3d transition metal-doped anatase TiO<sub>2</sub>. *Journal of Physics: Condensed Matter*. 2008. 20(12): 125207.
- [42] Hamal D.B. and Klabunde K.J. Synthesis, characterization, and visible light activity of new nanoparticle photocatalysts based on silver, carbon, and sulfur-doped TiO<sub>2</sub>. *Journal of Colloid and Interface Science*. 2007. 311(2): 514–22.
- [43] Biernat K. and Malinowski A. The Possibility of Future Biofuels Production Using Waste Carbon Dioxide and Solar Energy. 2013.

- [44] Dozzi M.V. and Selli E. Doping TiO<sub>2</sub> with p-block elements: Effects on photocatalytic activity. *Journal of Photochemistry and Photobiology C: Photochemistry Reviews*. 2013. 14(1): 13–28.
- [45] Ren W., Ai Z., Jia F., Zhang L., Fan X. and Zou Z. Low temperature preparation and visible light photocatalytic activity of mesoporous carbon-doped crystalline TiO<sub>2</sub>. *Applied Catalysis B: Environmental*. 2007. 69(3–4): 138–44.
- [46] Liu Q.-L., Zhao Z.-Y. and Liu Q.-J. Impact of sulfur-, tantalum-, or co-doping on the electronic structure of anatase titanium dioxide: A systematic density functional theory investigation. *Materials Science in Semiconductor Processing*. 2015. 33: 94–102.
- [47] Zaleska A. Characteristics of doped-TiO<sub>2</sub> photocatalysts. *Physicochemical Problems of Mineral Processing*. 2008. 42: 211–21.
- [48] Liu G., Han C., Pelaez M., Zhu D., Liao S., Likodimos V., Ioannidis N., Kontos A.G., Falaras P., Dunlop P.S.M., Byrne J.A. and Dionysiou D.D. Synthesis, characterization and photocatalytic evaluation of visible light activated C-doped TiO<sub>2</sub> nanoparticles. *Nanotechnology*. 2012. 23(29): 294003.
- [49] Zhang Z., Wang X., Long J., Gu Q., Ding Z. and Fu X. Nitrogen-doped titanium dioxide visible light photocatalyst: Spectroscopic identification of photoactive centers. *Journal of Catalysis*. 2010. 276(2): 201–14.
- [50] Kralova M., Dzik P., Vesely M. and Cihlar J. Preparation and characterization of doped titanium dioxide printed layers. *Catalysis Today*. 2014. 230: 188–96.
- [51] Gorska P., Zaleska a, Suska a and Hupka J. Photocatalytic Activity and Surface Properties of Carbon-Doped Titanium Dioxide. *Physicochemical Problems of Mineral Processing*. 2009. 43(43): 21–30.
- [52] Derjaguin B. V., Fedoseev D. V., Varnin V.P. and Vnukov S.P. The nature of metastable phases of carbon. *Nature*. 1977. 269: 398–9.
- [53] Di Valentin C., Pacchioni G. and Selloni A. Theory of carbon doping of titanium dioxide. *Chemistry of Materials*. 2005. 17(26): 6656–65.
- [54] Park J.-W., Kim D.-W., Seon H.-S., Kim K.-S. and Park D.-W. Synthesis of carbon-doped TiO<sub>2</sub> nanoparticles using CO<sub>2</sub> decomposition by thermal plasma. *Thin Solid Films*. 2010. 518(15): 4113–6.
- [55] Wu G., Nishikawa T., Ohtani B. and Chen A. Synthesis and Characterization of Carbon-Doped TiO<sub>2</sub> Nanostructures with Enhanced Visible Light Response. *Chemistry of Materials*. 2007. 19(18): 4530–7.



- [56] Parayil S.K., Kibombo H.S., Wu C.-M., Peng R., Baltrusaitis J. and Koodali R.T. Enhanced photocatalytic water splitting activity of carbon-modified TiO<sub>2</sub> composite materials synthesized by a green synthetic approach. *International Journal of Hydrogen Energy*. 2012. 37(10): 8257–67.
- [57] Tseng T.K., Lin Y.S., Chen Y.J. and Chu H. A review of photocatalysts prepared by sol-gel method for VOCs removal. *International Science of Molecular Sciences*. 2010. 11: 2336–61.
- [58] Chen Q.Y., Xue C., Li X.L. and Wang Y.H. Surfactant's effect on the photoactivity of Fe-doped TiO<sub>2</sub>. *Materials Science Forum*. 2013. 743–744: 367–71.
- [59] Li J., Yang X., Yu X., Xu L., Kang W., Yan W., Gao H., Liu Z. and Guo Y. Rare earth oxide-doped titania nanocomposites with enhanced photocatalytic activity towards the degradation of partially hydrolysis polyacrylamide. *Applied Surface Science*. 2009. 255(6): 3731–8.
- [60] Kuriechen S.K. and Murugesan S. Carbon-doped titanium dioxide nanoparticles mediated photocatalytic degradation of azo dyes under visible light. *Water, Air, & Soil Pollution*. 2013. 224(9): 1671.
- [61] Lu J., Wang Y., Huang J., Fei J., Cao L. and Li C. In situ synthesis of mesoporous C-doped TiO<sub>2</sub> single crystal with oxygen vacancy and its enhanced sunlight photocatalytic properties. *Dyes and Pigments*. 2017. 144: 203–11.
- [62] Shi J.-W., Chen J.-W., Cui H.-J., Fu M.-L., Luo H.-Y., Xu B. and Ye Z.-L. One template approach to synthesize C-doped titania hollow spheres with high visible-light photocatalytic activity. *Chemical Engineering Journal*. 2012. 195–196: 226–32.
- [63] Dong F., Wang H. and Wu Z. One-step “Green” synthetic approach for mesoporous C-doped titanium dioxide with efficient visible light photocatalytic activity. *Journal of Physical Chemistry C*. 2009. 113(38): 16717–23.
- [64] Shen M., Wu Z., Huang H., Du Y., Zou Z. and Yang P. Carbon-doped anatase TiO<sub>2</sub> obtained from TiC for photocatalysis under visible light irradiation. *Materials Letters*. 2006. 60(5): 693–7.
- [65] Lubis S., Yuliati L., Ling S., Sumpono I. and Nur H. Improvement of catalytic activity in styrene oxidation of carbon-coated titania by formation of porous carbon layer. *Chemical Engineering Journal*. 2012. 209: 486–93.
- [66] Lu X.H., Lei J., Zhou D., Fang S.Y., Dong Y.L. and Xia Q.H. Selective

- epoxidation of styrene with air over  $\text{Co}_3\text{O}_4\text{-MO}_x$  and  $\text{CoO}_x\text{-MO}_x/\text{SiO}_2$ . *Indian Journal of Chemistry*. 2010. 49(12): 1586–92.
- [67] Adam F. and Iqbal A. The oxidation of styrene by chromium-silica heterogeneous catalyst prepared from rice husk. *Chemical Engineering Journal*. 2010. 160(2): 742–50.
- [68] Liu J., Wang Z., Jian P. and Jian R. Highly selective oxidation of styrene to benzaldehyde over a tailor-made cobalt oxide encapsulated zeolite catalyst. *Journal of Colloid and Interface Science*. 2018. 517: 144–54.
- [69] Lubis S. Porous carbon-coated titania prepared by in-situ polymerization of styrene and its catalytic and photocatalytic activities in oxidation of alkenes. Universiti Teknologi Malaysia, Johor; 2013.
- [70] Lubis S. Porous carbon-coated Titania Prepared by in-situ Polymerization of Styrene and Its Catalytic and Photocatalytic Activities in Oxidation of Alkenes. Universiti Teknologi Malaysia; 2013.
- [71] Mohamed N.N. The preparation of averrhoa bilimbi-derived carbon-titania composite and its structure-function relationship in photocatalytic and catalytic reactions. Universiti Teknologi Malaysia; 2018.
- [72] Nyamukamba P., Tichagwa L. and Greyling C. The influence of carbon doping on  $\text{TiO}_2$  nanoparticle size, surface area, anatase to rutile phase transformation and photocatalytic activity. *Materials Science Forum*. 2012. 712: 49–63.
- [73] Yang X., Cao C., Erickson L., Hohn K., Maghirang R. and Klabunde K. Synthesis of visible-light-active  $\text{TiO}_2$ -based photocatalysts by carbon and nitrogen doping. *Journal of Catalysis*. 2008. 260(1): 128–33.
- [74] Yang X., Cao C., Hohn K., Erickson L., Maghirang R., Hamal D. and Klabunde K. Highly visible-light active C- and V-doped  $\text{TiO}_2$  for degradation of acetaldehyde. *Journal of Catalysis*. 2007. 252(2): 296–302.
- [75] Casino S., Di Lupo F., Francia C., Tuel A., Bodoardo S. and Gerbaldi C. Surfactant-assisted sol gel preparation of high-surface area mesoporous  $\text{TiO}_2$  nanocrystalline Li-ion battery anodes. *Journal of Alloys and Compounds*. 2014. 594: 114–21.
- [76] Uskokovic V. and Drogenik M. Synthesis of materials within reverse micelles. *Surface Review and Letters*. 2005. 12(2): 239–77.
- [77] Nur Adilah Hussien. Effects of carbon content on the photocatalytic activity of zinc oxide under visible light irradiation. 2019.

- [78] Parida K.M. and Sahu N. Visible light induced photocatalytic activity of rare earth titania nanocomposites. *Journal of Molecular Catalysis A: Chemical*. 2008. 287(1–2): 151–8.
- [79] Balantseva E., Camino B., Ferrari A.M. and Berlier G. Effect of post-synthesis treatments on the properties of ZnS nanoparticles: An experimental and computational study. *Oil and Gas Science and Technology*. 2015. 70(5): 817–29.
- [80] Pansamut G., Charinpanitkul T. and Suriyawong A. Removal of humic acid by photocatalytic process: Effect of light intensity. *Engineering Journal*. 2013. 17(3): 25–32.
- [81] Bloh J.Z. A holistic approach to model the kinetics of photocatalytic reactions. *Frontiers in Chemistry*. 2019. 7(March 2019): 1–13.
- [82] Park Y., Kim W., Park H., Tachikawa T., Majima T. and Choi W. Carbon-doped TiO<sub>2</sub> photocatalyst synthesized without using an external carbon precursor and the visible light activity. *Applied Catalysis B: Environmental*. 2009. 91: 355–61.
- [83] Simonsen M.E. and Søggaard E.G. Sol-gel reactions of titanium alkoxides and water : influence of pH and alkoxy group on cluster formation and properties of the resulting products. *Journal of Sol-Gel Science and Technology*. 2010. 53: 485–97.
- [84] Xie Y., Zhao X., Li Y., Zhao Q., Zhou X. and Yuan Q. CTAB-assisted synthesis of mesoporous F-N-codoped TiO<sub>2</sub> powders with high visible-light-driven catalytic activity and adsorption capacity. *Journal of Solid State Chemistry*. 2008. 181(8): 1936–42.
- [85] Liao D.L. and Liao B.Q. Shape, size and photocatalytic activity control of TiO<sub>2</sub> nanoparticles with surfactants. *Journal of Photochemistry and Photobiology A: Chemistry*. 2007. 187(2–3): 363–9.
- [86] Hanaor D.A.H. and Sorrell C.C. Review of the anatase to rutile phase transformation. *Journal of Materials Science*. 2011. 46(4): 855–74.
- [87] Mahshid S., Askari M. and Ghamsari M.S. Synthesis of TiO<sub>2</sub> nanoparticles by hydrolysis and peptization of titanium isopropoxide solution. *Journal of Materials Processing Technology*. 2007. 189: 296–300.
- [88] Kumar M.M., Badrinarayanan S. and Sastry M. Nanocrystalline TiO<sub>2</sub> studied by optical, FTIR and X-ray photoelectron spectroscopy: Correlation to presence

- of surface states. *Thin Solid Films*. 2000. 358(1): 122–30.
- [89] Shirke B.S., Korake P. V., Hankare P.P., Bamane S.R. and Garadkar K.M. Synthesis and characterization of pure anatase TiO<sub>2</sub> nanoparticles. *Journal of Materials Science: Materials in Electronics*. 2011. 22(7): 821–4.
- [90] Aware D. V and Jadhav S.S. Synthesis , characterization and photocatalytic applications of Zn-doped TiO<sub>2</sub> nanoparticles by sol–gel method. *Applied Nanoscience*. 2015. .
- [91] Liu Y., Zhao W. and Zhang X. Soft template synthesis of mesoporous Co<sub>3</sub>O<sub>4</sub>/RuO<sub>2</sub>.xH<sub>2</sub>O composites for electrochemical capacitors. *Electrochimica Acta* 53. 2008. 53: 3296–304.
- [92] Nur H. Modification of titanium surface species of titania by attachment of silica nanoparticles. *Materials Science and Engineering B*. 2006. 133: 49–54.
- [93] Astorino E., Peri J.B., Willey R.J. and Busca G. Spectroscopic Characterization of silicate-1 and titanium silicate-1. *Journal of Catalysis*. 1995. 157: 482–500.
- [94] Zecchina A., Bordiga S., Lamberti C., Ricchiardi G., Lamberti C., Ricchiardi G., Scarano D., Petrini G., Leofanti G. and Mantegazza M. Structural characterization of Ti centres in Ti-silicalite and reaction mechanisms in cyclohexanone ammoximation. *Catalysis Today*. 1996. 32: 97–106.
- [95] Jing L., Li S., Song S., Xue L. and Fu H. Investigation on the electron transfer between anatase and rutile in nano-sized TiO<sub>2</sub> by means of surface photovoltage technique and its effects on the photocatalytic activity. *Solar Energy Materials and Solar Cells*. 2008. 92(9): 1030–6.
- [96] De Haart L.G.J., De Vries A.J. and Blasse G. On the photoluminescence of semiconducting titanates applied in photoelectrochemical cells. *Journal of Solid State Chemistry*. 1985. 59: 291–300.
- [97] Serpone N., Lawless D. and Khairutdinovt R. Size effects on the photophysical properties of colloidal anatase TiO<sub>2</sub> particles: Size quantization or direct transitions in this indirect semiconductor? *Journal Physical Chemistry*. 1995. 99: 16646–54.
- [98] Sean N.A. The effect of calcination temperature on the structure-photocatalytic activity of carbon-doped titanium dioxide prepared via sol-gel route. Universiti Teknologi Malaysia; 2017.
- [99] Tripathi A.K., Mathpal M.C., Kumar P., Agrahari V., Singh M.K., Mishra S.K., Ahmad M.M. and Agarwal A. Photoluminescence and photoconductivity of ni

- doped titania nanoparticles. *Advanced Materials Letters*. 2015. 6(3): 201–8.
- [100] Kao L.H. and Chen Y.P. Characterization, photoelectrochemical properties, and surface wettabilities of transparent porous TiO<sub>2</sub> thin films. *Journal of Photochemistry and Photobiology A: Chemistry*. 2017. 340: 109–19.
- [101] Awoke T., Kuo C.J., Sorsa A., Pan C., Chen H., Meazah A., Cheng J., Su W. and Hwang B. Hybrid nanostructured microporous carbon-mesoporous carbon doped titanium dioxide / sulfur composite positive electrode materials for rechargeable lithium-sulfur batteries. *Journal of Power Sources*. 2016. 324: 239–52.
- [102] Xiao Q., Zhang J., Xiao C., Si Z. and Tan X. Solar photocatalytic degradation of methylene blue in carbon-doped TiO<sub>2</sub> nanoparticles suspension. *Solar Energy*. 2008. 82(8): 706–13.
- [103] Choi Y., Umebayashi T. and Yoshikawa M. Fabrication and characterization of C-doped anatase TiO<sub>2</sub> photocatalysts. *Journal of Materials Science*. 2004. 39(5): 1837–9.
- [104] Shao G.S., Liu L., Ma T.Y., Wang F.Y., Ren T.Z. and Yuan Z.Y. Synthesis and characterization of carbon-modified titania photocatalysts with a hierarchical meso-/macroporous structure. *Chemical Engineering Journal*. 2010. 160(1): 370–7.
- [105] Raja K.S., Misra M., Mahajan V.K., Gandhi T., Pillai P. and Mohapatra S.K. Photo-electrochemical hydrogen generation using band-gap modified nanotubular titanium oxide in solar light. *Journal of Power Sources*. 2006. 161(2): 1450–7.
- [106] Lim G.T., Kim K.H., Park J., Ohk S.H., Kim J.H. and Cho D.L. Synthesis of carbon-doped photocatalytic TiO<sub>2</sub> nano-powders by AFD process. *Journal of Industrial and Engineering Chemistry*. 2010. 16(5): 723–7.
- [107] Lachheb H., Guillard C., Lassoued H., Haddaji M., Rajah M. and Houas A. Photochemical oxidation of styrene in acetonitrile solution in presence of H<sub>2</sub>O<sub>2</sub> TiO<sub>2</sub>/H<sub>2</sub>O<sub>2</sub> and ZnO/H<sub>2</sub>O<sub>2</sub>. *Journal of Photochemistry and Photobiology A: Chemistry*. 2017. 346: 462–9.
- [108] Park H., Park Y., Kim W. and Choi W. Surface modification of TiO<sub>2</sub> photocatalyst for environmental applications. *Journal of Photochemistry and Photobiology C: Photochemistry Reviews*. 2013. 15(1): 1–20.
- [109] Foresman J.B. and Frisch A. Exploring Chemistry With Electronic Structure

- Methods [Internet]. *Gaussian, Inc.* 2013. 335 p.
- [110] Hehre W.J. A Guide to Molecular Mechanics and Quantum Chemical Calculations. 2003. 1–796 p.
- [111] Muscat J., Swamy V. and Harrison N.M. First-principles calculations of the phase stability of TiO<sub>2</sub>. *Physical Review B*. 2002. 65(22): 224112.
- [112] Kohanoff J. Electronic Structure Calculation for Solids and Molecules: Theory and Computational Methods. *Cambridge University Press*. 2006. 337 p.
- [113] Perdew J.P. and Ruzsinszky A. Understanding thomas-fermi-like approximations: Averaging over oscillating occupied orbitals. *Discrete and Continuous Dynamical Systems- Series A*. 2013. 33(11–12): 5319–25.
- [114] Grüning M., Gritsenko O. V. and Baerends E.J. Exchange-correlation energy and potential as approximate functionals of occupied and virtual Kohn–Sham orbitals: Application to dissociating H<sub>2</sub>. *The Journal of Chemical Physics*. 2003. 118(16): 7183.
- [115] Salzner U., Pickup P.G., Poirier R.A. and Lagowski J.B. Accurate method for obtaining band gaps in conducting polymers using a DFT/hybrid approach. *Journal of Physical Chemistry A*. 1998. 102(15): 2572–8.
- [116] Mewhort D.J.K., Cann N.M., Slater G.W. and Naughton T.J. High performance computing systems and applications. 2009. 418 p.
- [117] Albuquerque A.R., Garzim M.L., Santos I.M.G. Dos, Longo V., Longo E. and Sambrano J.R. DFT study with inclusion of the Grimme potential on anatase TiO<sub>2</sub>: structure, electronic, and vibrational analyses. *The journal of physical chemistry A*. 2012. 116(47): 11731–5.
- [118] Ouzzine M., Maciá-Agulló J.A., Lillo-Ródenas M.A., Quijada C. and Linares-Solano A. Synthesis of high surface area TiO<sub>2</sub> nanoparticles by mild acid treatment with HCl or HI for photocatalytic propene oxidation. *Applied Catalysis B: Environmental*. 2014. 154–155: 285–93.
- [119] Mogal S.I., Gandhi V.G., Mishra M., Tripathi S., Shripathi T., Joshi P.A. and Shah D.O. Single-step synthesis of silver-doped titanium dioxide: Influence of silver on structural, textural, and photocatalytic properties. *Industrial and Engineering Chemistry Research*. 2014. 53(14): 5749–58.
- [120] Matos J., García A., Zhao L. and Titirici M.M. Solvothermal carbon-doped TiO<sub>2</sub> photocatalyst for the enhanced methylene blue degradation under visible light. *Applied Catalysis A: General*. 2010. 390(1–2): 175–82.

- [121] Ding J., Yuan Y., Xu J., Deng J. and Guo J. TiO<sub>2</sub> nanopowder co-doped with iodine and boron to enhance visible-light photocatalytic activity. *Journal of Biomedical Nanotechnology*. 2009. 5(5): 521–7.
- [122] Elghniji K., Ksibi M. and Elaloui E. Sol–gel reverse micelle preparation and characterization of N-doped TiO<sub>2</sub>: Efficient photocatalytic degradation of methylene blue in water under visible light. *Journal of Industrial and Engineering Chemistry*. 2012. 18(1): 178–82.
- [123] Sano T., Mera N., Kanai Y., Nishimoto C., Tsutsui S., Hirakawa T. and Negishi N. Origin of visible-light activity of N-doped TiO<sub>2</sub> photocatalyst: Behaviors of N and S atoms in a wet N-doping process. *Applied Catalysis B: Environmental*. 2012. 128: 77–83.
- [124] Xiao H., Tahir-kheli J. and Goddard W.A. Accurate band gaps for semiconductors from density functional theory. *The Journal of Physical Chemistry Letters*. 2011. 2: 212–7.
- [125] Ko K.C., Lamiel-garcía O., Lee J.Y. and Illas F. Performance of a modified hybrid functional in the simultaneous description of stoichiometric and reduced TiO<sub>2</sub> polymorphs. *Physical chemistry chemical physics : PCCP*. 2016. 18(17): 12357–67.
- [126] Gao H., Ding C. and Dai D. Density functional characterization of C-doped anatase TiO<sub>2</sub> with different oxidation state. *Journal of Molecular Structure: THEOCHEM*. 2010. 944(1–3): 156–62.
- [127] Khan M., Cao W., Chen N., Usman Z., Khan D.F., Toufiq A.M. and Khaskheli M.A. Influence of tungsten doping concentration on the electronic and optical properties of anatase TiO<sub>2</sub>. *Current Applied Physics*. 2013. 13(7): 1376–82.
- [128] Lin Y., Zhu S., Jiang Z., Hu X., Zhang X., Zhu H., Fan J., Mei T. and Zhang G. Electronic and optical properties of S/I-codoped anatase TiO<sub>2</sub> from ab initio calculations. *Solid State Communications*. 2013. 171: 17–21.
- [129] Li M., Zhang J. and Zhang Y. Electronic structure and photocatalytic activity of N/Mo doped anatase TiO<sub>2</sub>. *Catalysis Communications*. 2012. 29: 175–9.
- [130] Peng L.P., Xu L. and Xia Z.C. Study the high photocatalytic activity of vanadium and phosphorus co-doped TiO<sub>2</sub> from experiment and DFT calculations. *Computational Materials Science*. 2014. 83: 309–17.
- [131] Pan G., Xuejun Z., Wenfang Z., Jing W. and Qingju L. First-principle study on anatase TiO<sub>2</sub> codoped with nitrogen and ytterbium. *Journal of Semiconductors*.

2010. 31(3): 032001.
- [132] Tsuneda T. and Hirao K. Self-interaction corrections in density functional theory. *Journal of Chemical Physics*. 2014. 140(18).
- [133] Bao J.L., Gagliardi L. and Truhlar D.G. Self-interaction error in density functional theory: An appraisal. *Journal of Physical Chemistry Letters*. 2018. 9(9): 2353–8.
- [134] Mori-Sánchez P., Cohen A.J. and Yang W. Localization and delocalization errors in density functional theory and implications for band-gap prediction. *Physical Review Letters*. 2008. 100(146401): 1–4.
- [135] Di Valentin C. and Pacchioni G. Trends in non-metal doping of anatase TiO<sub>2</sub>: B, C, N and F. *Catalysis Today*. 2013. 206: 12–8.
- [136] Labat F., Baranek P., Domain C., Minot C. and Adamo C. Density functional theory analysis of the structural and electronic properties of TiO<sub>2</sub> rutile and anatase polytypes: Performances of different exchange-correlation functionals. *The Journal of Chemical Physics*. 2007. 126(15): 154703.
- [137] Grimme S. and Neese F. Double-hybrid density functional theory for excited electronic states of molecules. *Journal of Chemical Physics*. 2007. 127(154116): 1–18.
- [138] Nagare B.J., Jaware S., Habale D. and Chavan S. First-principles calculations of electronic and magnetic properties of carbon doped TiO<sub>2</sub> clusters. *Computational Materials Science*. 2013. 68: 127–31.
- [139] Yu D., Zhou W., Liu Y., Zhou B. and Wu P. Density functional theory study of the structural, electronic and optical properties of C-doped anatase TiO<sub>2</sub> (101) surface. *Physics Letters A*. 2015. 379(28–29): 1666–70.
- [140] Xi X., Dong P., Pei H., Hou G., Zhang Q., Guan R., Xu N. and Wang Y. Density functional study of X monodoped and codoped (X = C, N, S, F) anatase TiO<sub>2</sub>. *Computational Materials Science*. 2014. 93: 1–5.
- [141] Zhukov V.P., Shein I.R. and Zainullina V.M. Electronic band structure, optical absorption and photocatalytic activity of anatase doped with bismuth or carbon. *Journal of Alloys and Compounds*. 2013. 548(9): 46–51.
- [142] Frisch M.J., Trucks G.W., Schlegel H.B., Scuseria G.E., Robb M.A., Cheeseman J.R. et al. Gaussian 09, Revision C.01. 2010.
- [143] Roothan C.C.J. New developments in molecular orbital theory. *Reviews of Modern Physics*. 1951. 23(2): 69–89.



- [144] Becke A.D. Density-Functional thermochemistry. III. The role of exact exchange. *Journal of Chemical Physics*. 1993. 98(7): 5648–52.
- [145] Lee C., Yang W. and Parr R.G. Development of the Colle-Salvetti correlation-energy formula into a functional of the electron density. *Physical Review B*. 1988. 37(2): 785–9.
- [146] Miehlich B., Savin A., Stoll H. and Preuss H. Results obtained with the correlation energy density functionals of Becke and Lee, Yang and Parr. *Chemical Physics Letters*. 1989. 157(3): 200–6.
- [147] Perdew J.P., Chevary J.A., Vosko S.H., Jackson K.A., Pederson M.R., Singh D.J. and Fiolhais C. Atoms, molecules, solids, and surfaces: Applications of the generalized gradient approximation for exchange and correlation. *Vol. 46, Physical Review B*. 1992. p. 6671–87.
- [148] Shi J.M., Peeters F.M., Hai G.Q. and Devreese J.T. Donor transition energy in GaAs superlattices in a magnetic field along the growth axis. *Physical Review B*. 1991. 44(11): 5692–702.
- [149] Perdew J.P., Burke K. and Ernzerhof M. Generalized gradient approximation made simple. *Physical Review Letters*. 1996. 77(18): 3865–8.
- [150] Perdew J.P., Burke K. and Ernzerhof M. Errata: Generalized gradient approximation made simple. *Physical Review Letters*. 1997. 78(7): 1396.
- [151] Adamo C. and Barone V. Toward reliable density functional methods without adjustable parameters: The PBE0 model. *Journal of Chemical Physics*. 1999. 110(13): 6158–70.
- [152] Ernzerhof M. and Perdew J.P. Generalized gradient approximation to the angle- and system-averaged exchange hole. *Journal of Chemical Physics*. 1998. 109(9): 3313–20.
- [153] Schwabe T. and Grimme S. Double-hybrid density functionals with long-range dispersion corrections: higher accuracy and extended applicability. *Physical chemistry chemical physics : PCCP*. 2007. 9: 3397–406.
- [154] Frisch M.J., Head-Gordon M. and Pople J.A. Semi-direct algorithms for the MP2 energy and gradient. *Chemical Physics Letters*. 1990. 166(3): 281–9.
- [155] Head-Gordon M., Pople J.A. and Frisch M.J. MP2 energy evaluation by direct methods. *Chemical Physics Letters*. 1988. 153(6): 503–6.
- [156] Sæbø S. and Almlöf J. Avoiding the integral storage bottleneck in LCAO calculations of electron correlation. *Chemical Physics Letters*. 1989. 154(1):

83–9.

- [157] Head-Gordon M. and Head-Gordon T. Analytic MP2 frequencies without fifth-order storage. Theory and application to bifurcated hydrogen bonds in the water hexamer. *Chemical Physics Letters*. 1994. 220(1–2): 122–8.
- [158] Parra R.D. and Farrell H.H. Binding energy of metal oxide nanoparticles. *The Journal of Physical Chemistry C*. 2009. 113(12): 4786–91.
- [159] Housecroft C.E. and Sharpe A.G. Chapter 3: An introduction to molecular symmetry. In: *Inorganic Chemistry*. 2010. p. 98.
- [160] Zhu H.X. and Liu J.-M. Electronic and optical properties of C and Nb co-doped anatase TiO<sub>2</sub>. *Computational Materials Science*. 2014. 85: 164–71.
- [161] Zheng X., Cohen A.J., Mori-Sánchez P., Hu X. and Yang W. Improving band gap prediction in density functional theory from molecules to solids. *Physical Review Letters*. 2011. 107(2): 1–4.
- [162] Hua Gui Y., Cheng Hua S., Shi Zhang Q., Jin Z., Gang L., Sean Campbell S., Hui Ming C. and Gao Qing L. Anatase TiO<sub>2</sub> single crystals with a large percentage of reactive facets. *Nature*. 2008. 453(7195): 638–41.
- [163] Erdin S., Lin Y., Halley J.W., Zapol P., Redfern P. and Curtiss L. Self-consistent tight binding molecular dynamics study of TiO<sub>2</sub> nanoclusters in water. *Journal of Electroanalytical Chemistry*. 2007. 607: 147–57.
- [164] Lazzeri M., Vittadini A. and Selloni A. Structure and energetics of stoichiometric TiO<sub>2</sub> anatase surfaces. *Physical Review B*. 2001. 63(155409): 1–9.
- [165] Glassford K.M. and Chelikowsky J.R. Structural and electronic properties of titanium dioxide. *Physical Review B*. 1992. 46(3): 1284–98.
- [166] Gangadharan R.P. and Krishnan, S S. Natural bond orbital (NBO) population analysis of 1-Azanaphthalene-8-ol. *Acta Physica Polonica A*. 2014. 125(1): 18–22.
- [167] Zhang R., Wang Q., Li Q., Dai J. and Huang D. First-principle calculations on optical properties of CN-doped and CN-codoped anatase TiO<sub>2</sub>. *Physica B: Condensed Matter*. 2011. 406(18): 3417–22.
- [168] Glasser L. and Sheppard D.A. Cohesive Energies and Enthalpies: Complexities, Confusions, and Corrections. *Inorganic Chemistry*. 2016. 55(14): 7103–10.
- [169] Eltermann M., Utt K., Lange S. and Jaaniso R. Sm<sup>3+</sup> doped TiO<sub>2</sub> as optical oxygen sensor material. *Optical Materials*. 2016. 51: 24–30.

- [170] Wu H.-C., Lin S.-W. and Wu J.-S. Effects of nitrogen concentration on N-doped anatase TiO<sub>2</sub>: Density functional theory and Hubbard U analysis. *Journal of Alloys and Compounds*. 2012. 522: 46–50.
- [171] Wang Y., Zhang R., Li J., Li L. and Lin S. First-principles study on transition metal-doped anatase TiO<sub>2</sub>. *Nanoscale Research Letters*. 2014. 9(1): 46.
- [172] Bai Y. and Wang D. Fundamentals of fuzzy logic control – Fuzzy sets , fuzzy rules and defuzzifications. In: *Advanced Fuzzy Logic Technologies in Industrial Applications*. 2006.
- [173] Sunitha M.S. and Mathew S. Fuzzy graph theory: A survey. *Annals of Pure and Applied Mathematics*. 2013. 4(1): 92–110.
- [174] Samanta S., Sarkar B., Shin D. and Pal M. Completeness and regularity of generalized fuzzy graphs. *SpringerPlus*. 2016. 5(1).
- [175] Hassan N. and Ahmad T. A review on taxonomy of fuzzy graph. *Malaysian Journal of Fundamental and Applied Sciences*. 2017. 13(1): 6–13.
- [176] Ahmad T., Baharun S. and Arshad K.A. Modeling a clinical incineration process using fuzzy autocatalytic set. *Journal of Mathematical Chemistry*. 2010. 47(4): 1263–73.
- [177] Harish N.A., Ismail R. and Ahmad T. Transformation of fuzzy state space model of a boiler system: A graph theoretic approach. *WSEAS Transactions on Mathematics*. 2010. 9(9): 669–78.
- [178] Sivaranjani K. Synthesis, characterization and application of hetero atom doped mesoporous TiO<sub>2</sub>. National Chemical Laboratory Pune, India; 2012.
- [179] Bettinelli M., Dallacasa V., Falcomer D., Fornasiero P., Gombac V., Montini T., Romanò L. and Speghini a. Photocatalytic activity of TiO<sub>2</sub> doped with boron and vanadium. *Journal of Hazardous Materials*. 2007. 146(3): 529–34.
- [180] Moghaddam H.M. and Nasirian S. Dependence of activation energy and lattice strain on TiO<sub>2</sub> nanoparticles? *Nanoscience Methods*. 2012. .
- [181] Lettmann C., Hildenbrand K., Kisch H., Macyk W. and Maier W.F. Visible light photodegradation of 4-chlorophenol with a coke-containing titanium dioxide photocatalyst. *Applied Catalysis B: Environmental*. 2001. 32(4): 215–27.
- [182] Zhukov V.P. and Zainullina V.M. The effect of crystal lattice distortions on the electronic band structure and optical properties of the N,V- and N,Na-doped anatase. *Physica B: Condensed Matter*. 2011. 406(19): 3752–8.
- [183] Li X., Gao H. and Liu G. A LDA+U study of the hybrid graphene/anatase TiO<sub>2</sub>

- nanocomposites: Interfacial properties and visible light response. *Computational and Theoretical Chemistry*. 2013. 1025: 30–4.
- [184] Adán C., Bahamonde A., Oller I., Malato S. and Martínez-Arias A. Influence of iron leaching and oxidizing agent employed on solar photodegradation of phenol over nanostructured iron-doped titania catalysts. *Applied Catalysis B: Environmental*. 2014. 144(1): 269–76.
- [185] Zhu Y., Wei W., Dai Y. and Huang B. Tuning electronic structure and photocatalytic properties by Ag incorporated on (0 0 1) surface of anatase TiO<sub>2</sub>. *Applied Surface Science*. 2012. 258(10): 4806–12.
- [186] Karbassi M., Nemati A., Hossinie Zari M. and Ahadi K. Effect of iron oxide and silica doping on microstructure, bandgap and photocatalytic properties of titania by water-in-oil microemulsion technique. *Transactions of the Indian Ceramic Society*. 2011. 70(4): 227–32.
- [187] Kohtani S., Kawashima A. and Miyabe H. Reactivity of trapped and accumulated electrons in titanium dioxide photocatalysis. *Catalysts*. 2017. 7(10).

## LIST OF PUBLICATIONS

1. Siti Hajar Alias, Nurul Najidah Mohamed, Leaw Wai Loon and Sheela Chandren (2019). Synthesis of carbon-doped titanium dioxide and its activity in the photocatalytic oxidation of styrene under visible light irradiation, *Malaysian Journal of Fundamental and Applied Sciences*, 15(1), 291-297. **(Indexed by Clarivate Analytics).**